Analytica Chimica Acta 1251 (2023) 340976

Contents lists available at ScienceDirect

Analytica Chimica Acta

journal homepage: www.elsevier.com/locate/aca

Single-cell HER2 quantification via instant signal amplification in microdroplets

Xiaoxian Liu [a,b,1], Yifan Zhu [a,b,1], Caoxin Li [a,b,1], Yanyun Fang [c], Jinna Chen [d], Fei Xu [a], Yanqing Lu [a], Perry Ping Shum [d], Ying Liu [c,*], Guanghui Wang [a,b,**]

[a] College of Engineering and Applied Sciences, Nanjing University, Jiangsu, 210093, China
[b] Key Laboratory of Intelligent Optical Sensing and Integration of the Ministry of Education, Nanjing University, Jiangsu, 210009, China
[c] School of Chemistry and Chemical Engineering, Nanjing University, Jiangsu, 210093, China
[d] Department of Electrical and Electronics Engineer, Southern University of Science and Technology, Shenzhen, 518055, China

HIGHLIGHTS

- Cation exchange combined with droplet microfluidic amplifies fluorescence signal.
- Uniform luminescence of Rhod-5N in droplets improves sensitivity and accuracy.
- Tapered capillary bundle directly input regents and instant generated tiny droplets.
- HER2 protein molecules of sk-br-3 cells were quantified as 9.795 × 10^6–2.038 × 10^5.

GRAPHICAL ABSTRACT

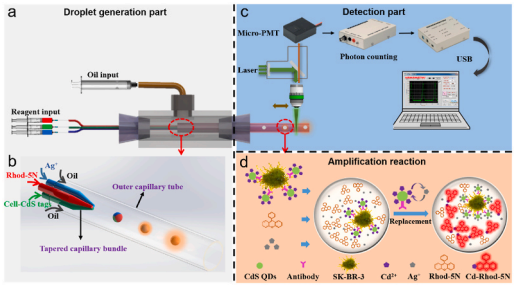

ARTICLE INFO

Handling Editor: Professor Chuck Henry

Keywords:
Droplet microfluidics
Instant cation exchange signal amplification
HER2 protein expression
Single-cell
Quantitative detection

ABSTRACT

Accurate and ultrasensitive evaluation of human epidermal growth factor receptor 2 (HER2) protein is key to early diagnosis and subtype differentiation of breast cancer. Single-cell analyses to reduce ineffective targeted therapies due to breast cancer heterogeneity and improve patient survival remain challenging. Herein, we reported a novel droplet microfluidic combined with an instant cation exchange signal amplification strategy for quantitative analysis of HER2 protein expression on single cells. In the 160 μm droplets produced by a tapered capillary bundle, abundant Immuno-CdS labeled on HER2-positive cells were replaced by Ag^+ to obtain Cd^{2+} that stimulated Rhod-5N fluorescence. This uniformly distributed and instantaneous fluorescence amplification strategy in droplets improves sensitivity and reduces signal fluctuation. Using HER2 modified PS microsphere to simulate single cells, we obtained a linear fitting of HER2-modified concentration and fluorescence intensity in microdroplets with the limit detection of 11.372 pg mL^{-1}. Moreover, the relative standard deviation (RSD) was 4.2-fold lower than the traditional immunofluorescence technique (2.89% vs 12.21%). The HER2 protein on SK-BR-3 cells encapsulated in droplets was subsequently quantified, ranging from 9862.954 pg mL^{-1} and 205.26 pg mL^{-1}, equivalent to 9.795 × 10^6 and 2.038 × 10^5 protein molecules. This detection system provides a universal platform for single-cell sensitive quantitative analysis and contributes to the evaluation of HER2-positive tumors.

* Corresponding author.
** Corresponding author. College of Engineering and Applied Sciences, Nanjing University, Jiangsu, 210093, China.
E-mail addresses: yingliu@nju.edu.cn (Y. Liu), wangguanghui@nju.edu.cn (G. Wang).
[1] These authors Xiaoxian Liu, Yifan Zhu, and Caoxin Li contributed equally to this work.

https://doi.org/10.1016/j.aca.2023.340976
Received 16 January 2023; Received in revised form 11 February 2023; Accepted 13 February 2023
Available online 20 February 2023
0003-2670/© 2023 Elsevier B.V. All rights reserved.

1. Introduction

According to the latest global cancer data reported by the WHO's International Agency for Research on Cancer (IARC) in 2021, the number of new cases of breast cancer in women was 2.3 million (11.7%), overtaking lung cancer as the most common cancer [1]. But, breast cancer mortality has slowly declined in the past decade due to advances in early detection and targeted therapies [2]. Human epidermal growth factor receptor 2 (HER2) is a transmembrane protein with tyrosine kinase activity, whose overexpression plays an important role in the tumorigenesis and invasion of the cancer cell. In accordance with St. Gallen/Vienna 2021 consensus, in addition to being an important clinical biomarker for targeted therapy [3], subtype identification and prognostic strategy selection for early breast cancer could be guided by HER2 protein [4]. Early detection of HER2 protein can effectively improve the survival rate of HER2-positive patients [5–7].

The current HER2 protein detection method is mainly done by invasive tumor biopsy using immunohistochemistry (IHC) and gold standard fluorescence in situ hybridization (FISH) [8,9]. But these two methods are dependent on fluorescence staining of the section pathological analysis, which is time-consuming, semi-quantitative, and cannot directly detect the protein marker levels in patients after surgical treatment or in patients with recurrent and metastatic tumors. Additionally, cancer cell heterogeneity also poses a challenge in evaluating the efficacy of HER2-targeted therapy [10]. The emergence of single-cell quantization has provided critical insights into solving this problem. Fluorescence flow cytometry (FCM) is the current benchmark for single cell protein expression characterization with high efficiency in locating and counting protein on the surface of individual cells in large heterogeneous populations [11]. However, the quantitative fluorescence signal after staining cells with fluorescence-labeled antibodies is highly dependent on the spontaneous fluorescence intensity, which is easily indistinguishable from noise signals and impurities in the sample solution when detecting trace proteins, limiting the sensitivity [12,13]. And the equipment is expensive and requires skilled personnel to operate [14]. Hence, there is an urgent need for a portable, fluorescent-amplified, ultrasensitive quantitative assay strategy to precisely identify HER2 protein expression levels in single cells.

As an efficient point-of-care-testing (POCT) tool, microfluidic has gained certain attention in the field of single-cell analysis due to its advantages of high throughput and sensitivity, integration, automation, and low consumption [15–19]. However, mixing homogeneous fluids is difficult and prone to cross-contamination in traditional microfluidics. Droplet-based microfluidics is an emerging technology developed in recent years, that has been proved to be applicable for single-cell proteomic analysis, genetic analysis, and screening [20–23]. The internal reaction environment of droplets is stable and very localized, which could use to encapsulate single cells for individual inspection, providing an isolated environment within the pL level and eliminating the interference of environment and nonspecific cells [24–26]. Capillary-assisted droplet microfluidic enables convenient, monodisperse, long-term single-cell encapsulation and real-time analysis of droplets by using simple pipette injection [27,28]. Moreover, the construction of multibarrel capillary bundle structures is more conducive to the simultaneous formation and coalescence of droplets by simple digital adjustment, which has obvious advantages for the generation of droplets with controllable morphology and composition [29,30]. This method eliminates the pre-mixing of multiple reagents before droplet generation and provides a new strategy for instantaneous reaction cases. However, each channel of multibarrel capillary bundle relay on extra Teflon tubing inserted for reagent input limited the size of tapered tip (usually a few hundred μm) and the size of generated droplet. Meanwhile, the heterogeneity of droplet size is still a struggle for the capillary assisted droplet microfluidic, which affects the accuracy of single-cell detection.

The cation exchange reaction is an instantaneous conversion process that replaces cation in the ionic nanocrystal with another cation while keeping the structural framework [31–33]. The strategy of ionic nanocrystals releasing a large number of cations by Ag^+ replacement and combining with cationic responsive fluorescent dye to amplify the signal has been proven to be applicable for cancer cells, protein, and miRNA detection [34–37]. At this point, instantaneous reaction avoids fluorescence quenching phenomenon. Moreover, the fluorescence reporter molecules are evenly distributed in the detection solution avoiding the detection error caused by the random position of the target analyte. Compared with ordinary fluorescence detection methods, the cation exchange reaction shows superiority in rapid and ultrasensitive detection of trace targets, which is particularly suitable for single-cell level detection [38].

In this paper, we presented a high-throughput flow HER2 protein quantification strategy for a single breast cancer cell via cation exchange fluorescence signal amplification reaction in microdroplets. The Ag^+, Rhod-5N, and Immuno-CdS-cell complex mixture solution for the reaction were simultaneously injected into a hydrophobic capillary bundle structure to generate droplets of uniform size after instantaneous mixing. All Cd^{2+} participating in the composition of CdS quantum dots (QDs) were replaced instantaneously by Ag^+ and coordinated with Rhod-5N to generate intensity fluorescence in whole droplets, which enhanced the detection sensitivity and repeatability. Furthermore, combined with the characteristics that the micro- (photomultiplier tube) PMT-based detection equipment can move flexibly along the output channel, the fluorescence signal can be recorded at the completion of the instantaneous cation exchange reaction, reducing the impact of long-term contact between cells and reagents. The experimental dose of each droplet is relatively fixed by capillary bundle injection, and the fluorescence signal contrast of cell or not can be obtained without the separation and collection of cations exchanged. Quantitative detection of HER2 protein in a single cell was realized by recording the fluorescence intensity of various concentrations of HER2 protein immobilized on a single microsphere surface. The sensitivity of the proposed strategy for HER2 protein was 11.372 pg mL^{-1}, and the amount of surface HER2 protein in single cells we detected can be calculated by the linear fit, corresponding 9.795×10^6 and 2.038×10^5 biomarker protein molecules. To our knowledge, there is no report on the detection of HER2 protein in single cells by cation exchange amplification fluorescence reaction using droplet microfluidic. This strategy demonstrates good application potential in ultrasensitive detection of trace substances in single cells and differentiation of tumor heterogeneity.

2. Experimental

2.1. Reagents and instruments

Cadmium chloride ($CdCl_2{\cdot}5H_2O$) and N-Hydroxysulfosuccinimide sodium salt (NHS) was obtained from Alfa Aesar (Shanghai, China). Rhodamine5N (Rhod-5N), 3-mercaptopropionic acid (MPA, 99%), Mineral continuous, ethanesulfonic acid (MES), and Carboxylated Polystyrene microspheres (PS–COOH) (catalog #P107813) were purchased from Aladdin Reagent Co., Ltd. (Shanghai, China). Silver nitrate (99%), N-(3-dimethylaminopropyl)-N′-ethylcarbodiimide hydrochloride (EDC), and PBS buffer (pH7.4) were purchased from Sigma-Aldrich (Shanghai, China). Tween-20 was purchased from Sinopharm Chemical Reagent Co., Ltd (China). Mouse monoclonal Anti-HER2 antibody (catalog #10004-MM03), Anti-HER2 antibody (Biotin) (catalog #10004-MM01-B), and Human HER2 protein (catalog #10004-H02H) was purchased from Sino Biological Inc (China). Streptavidin/FITC (catalog #SF068) were provided by Solarbio (Beijing, China). Quartz tube (600 μm inner diameter, 950 μm outer diameter) was purchased from Guanghua Quartz Glass Co., Ltd (Jinzhou, China). Capillary (320 μm inner diameter) (catalog #YN-320450) was purchased from Nuoheng Optical Cable Co., Ltd (Handan, China). Micro-photomultiplier tube (PMT) modules H12402 were purchased from Hamamatsu (Japan).

Microscopy images of droplets was obtained by Olympus BX51

fluorescence microscope with a 10 × objective (Olympus, Japan). The fluorescence microscopy images were captured by Olympus BX51 with a modified Olympus U-MWG2 fluorescent module: excitation 473–491 nm, emission filter 502.5–547.5 nm, and a dichroic mirror: reflection band: 350–491 nm, transmission band: 497.8–900 nm. Scanning electron microscope (SEM) images of tapered capillary bundle were characterized via an ULTRA 55 microscope (ZEISS, Germany). The zeta potential values of Immuno-CdS tags and Immuno-PS microspheres, and the DLS measurement of Immuno-CdS tags were recorded on Litesizer 500 (Anto paar, Austria). Nicolet iS10 (Thermo Fisher, USA) was used to record FITR spectra.

2.2. Fabrication of Immuno-CdS tags

First, the MPA-CdS QDs were prepared via disulfide reduction and sulfhydryl amine coupling [39]. The detailed synthesis process was described in S1. Subsequently, monodispersed CdS QDs nanoparticles with surface carboxyl groups (50 mg mL^{-1}) were activated by 0.1 M EDC and NHS in 500 μL 0.1 M MES buffer (pH 5.5) at 37 °C for 30 min. 5 μg antibodies (Anti-HER2 antibodies) were hotheaded to incubated with activated CdS QDs for 2.5 h under shaking. The un-conjugated antibodies were removed by centrifugation and the un-reacted carboxyl groups on the surface of CdS QDs were blocked by 1% BSA for 1 h. The as-prepared Immuno-CdS tags were resuspended in 500 μL PBST solution (pH 7.4, 0.05% Tween-20) and stored at 4 °C for further use [40].

2.3. Assembly of the droplet generation chip

As shown in Fig. S2a, the designed co-flowing droplet generation chip consists of five parts: a 3-mm diameter Teflon hose, a tapered capillary bundle containing three capillaries stretched to 20 μm inner diameter (The preparation method was illustrated in detail in S2), a pre-hydrophobic quartz tube with 700 μm inner diameter, a cover plate (length 41 mm × 26 mm width), and a liquid chamber (length 50 mm × 40 mm width) with three slots with diameters of 1 μm, 2 μm, and 3 μm, respectively. Polymethyl methacrylate (PMMA) materials were processed into the cover plate and liquid chamber by using a CNC machine. Then, the capillary bundle, advanced hydrophobic quartz tube and Teflon hose were embedded in the corresponding slots as reagent adding channel, droplet output channel and continuous input channel, respectively. The transparent PMMA plate was covered on top of the device for sealing off continuous phase and observing of droplets generation (Fig. S2b (i)). The UV curing adhesive was used to seal each joint. Notable, the capillary bundle was suspended in the center of quartz tube in the real assembled droplet generation chip shown in Fig. S2b (ii).

2.4. Establishment of real-time fluorescence signal detection platform

An excitation laser beam with a wavelength of 532 nm is focused on the continuously moving droplets within the output channel. At the same time, the emission fluorescent signal with a wavelength around 577 nm is collected by an objective (Olympus MPlanFL N20X/0.45) and guided into micro-PMT modules (Hamamatsu H12402) for high-sensitivity photoelectric sensing detection. The electrical signal from the PM detector was connected to the Hamamatsu photon counter system with a 50 μs of minimum sampling interval and a 50 μA lm^{-1} of minimum luminous sensitivity.

2.5. Cell culture

The SK-BR-3 (human breast adenocarcinoma cells) were purchased from ATCC and cultured in DMEM supplemented containing 10% FBS, 100 IU mL^{-1} of penicillin, and 100 mg mL^{-1} of streptomycin at 37 °C in a humidified incubator with 5% CO_2. After digestion with trypsin (wt 0.25%) for 2 min, fresh culture medium was added to obtain the cell suspension. Cells were collected by centrifugation at 1000 rpm for 5 min and resuspended by PBS buffer for counting (1.14×10^7 cells mL^{-1}) and immediately use.

3. Results and discussion

3.1. Principle of the instant signal amplification-based droplet microfluidic for single-cell HER2 detection

Fig. 1 illustrates the structural composition and operation principle of the proposed droplet microfluidic system for single breast cancer cell detection. To achieve the instantaneous and ultrasensitive detection of HER2 protein in single cells, we introduced the cation exchange signal amplification strategy based on MPA-CdS QDs into the droplets as an alternative to conventional fluorescent labeling with the characteristic of uniform luminescence in droplet. Firstly, anti-HER2 antibodies modified CdS attached rapidly and in large quantities to the surface of breast cancer cells, forming the immuno-CdS-cell complex structure. Then, a $AgNO_3$ solution, a Rhod-5N, and the diluted complex were synchronized injected into the tapered capillary bundle of the designed droplet generation chip, respectively. Under the limitation of the diameter of the tapered end of the capillary bundle, homogeneous microdroplets that encapsulated single cells were formed in succession when the flow of capillary bundle met a continuous phase from the vertical direction capillary at the device cavity. As the droplets continued to flow through the output glass tube for a few seconds, thousands of Cd^{2+} were instantaneously released by Ag^{+} and reacted with Rhod-5N to generate an intensive fluorescence signal at 532 nm excitation wavelength. Finally, the amplified fluorescent signal was measured using a photon counter system with a micro-PMT module and used for real-time and quantitative analysis of single-cell HER2 protein.

3.2. Characterization of immuno-CdS tags

As characterized in Fig. 2a of transmission electron microscopy (TEM) image, the average size of aqueous synthesis of CdS QDs using MPA as stabilizer was 4 nm in diameter. Powder X-ray diffraction (XRD) was used to confirm the crystal structure and phase purity of the main synthetic product. Fig. 2b shows the typical XRD pattern of the CdS nanoparticles. The diffraction peaks at 2θ values of 26.45°, 43.87°, 51.96°, and 70.3° refer to (111), (220), (311), and (331) planes of CdS cubic sphalerite structure, respectively, which could all be indexed to the standard PDF card (JCPDS No. 65–2887). Under excitation light of 365 nm, the synthetic CdS QDs exhibit red fluorescence with an emission peak at ~670 nm in Fig. 2c. HER2 antibody was directly modified onto the CdS QDs surface due to the abundant activated carboxyl group via the EDC/NHS-based coupling reaction to specific recognized HER2 high expression cells. Fig. 2d displayed the Fourier transform infrared (FTIR) spectroscopy results revealed that HER2 antibody had been conjugated onto the CdS surface. The dynamic light scattering (DLS) and Zeta potential results in Fig. S3 also confirmed the successful fabrication of the immuno-CdS tags with the average diameter of CdS QDs increased from 4 nm to 11 nm and the zeta potential value of CdS changes from −8.2 mV to −29.6 mV after antibody modification.

3.3. Optimization of the instant signal amplification in microdroplets

As a dual functional tag in the droplet detection system, the immuno-CdS tags contributed to specific binding to target breast cancer cells and providing Cd^{2+} for fluorescence signal amplification in droplets. Successful cation exchange reaction is a significant factor in improving the sensitivity of droplet microfluidic flow detection systems. We investigated the fluorescence signals of 500 μM $AgNO_3$ and 2 μM Rhod-5N mixture in the presence and absence of Cd^{2+} in a droplet. As shown in Fig. 3a, the fluorescence signals in the presence of Immuno-CdS tags were increased ~9.71 fold on average. Fig. 3b revealed the cation exchange fluorescence intensity increased linearly with the Cd^{2+}

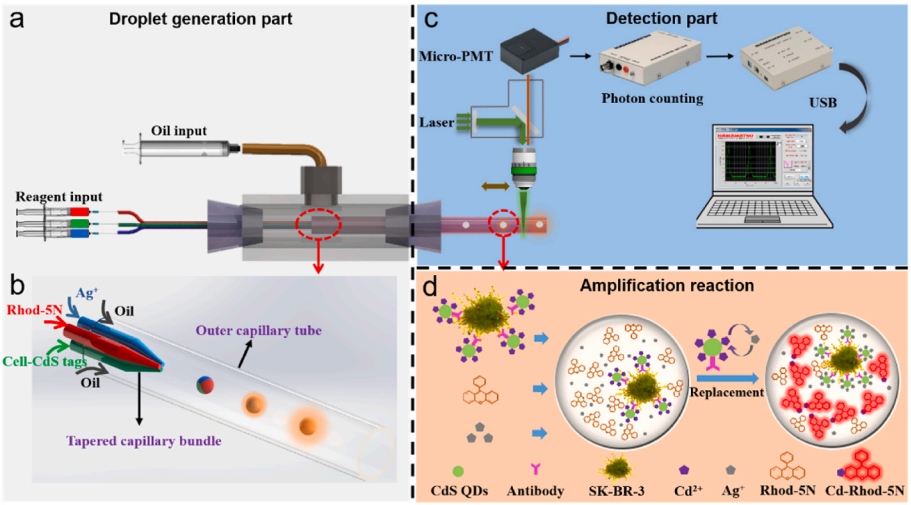

Fig. 1. Schematic diagram of the instant signal amplification-based droplet microfluidic, including four parts: a) the droplet generation unit, the b) detail of the tapered capillary bundle structure in droplet generation unit, c) Micro-photomultiplier tube (PMT) detection part, d) the principle of cation amplification reaction in a droplet.

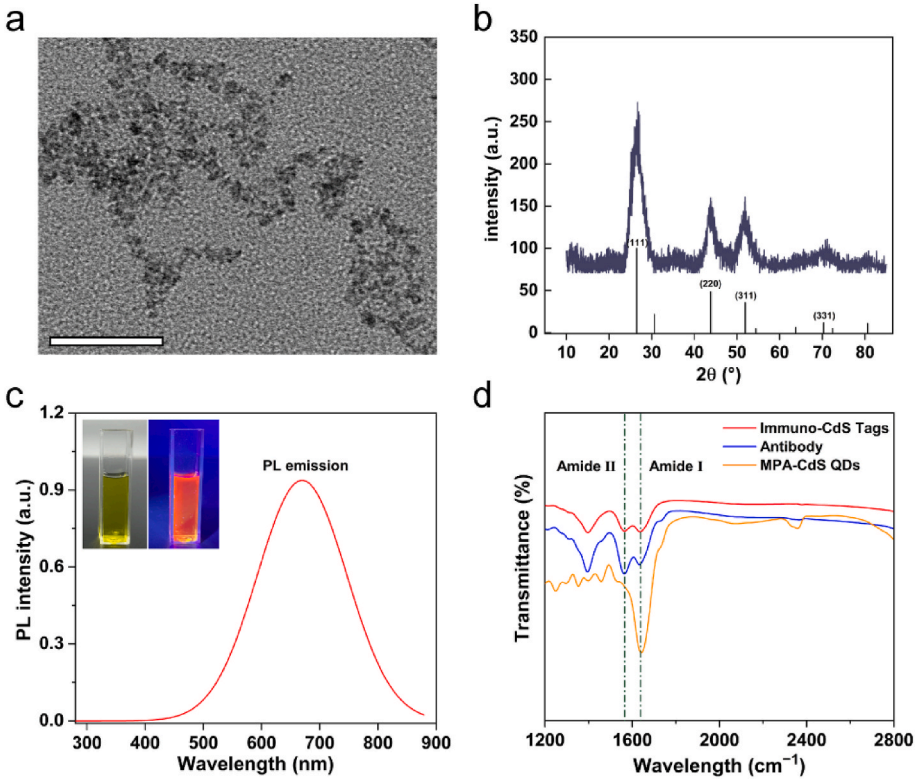

Fig. 2. a) TEM images of CdS (scale bar: 50 nm). b) Typical XRD patterns of CdS. The bottom solid lines are the planes of the standard PDF card (JCPDS No. 65–2887). c) Fluorescence emission spectrum (λ_{ex} = 365 nm) of CdS. Insert shows the photographs of CdS under visible light and 365 nm UV light. d) FITR spectra of MPA-CdS QDs (orange line), antibody (blue line), and immuno-CdS Tags (red line). The characteristic absorption peaks of protein amide band I (1640 cm^{-1}) and II (1561 cm^{-1}) were shown in immuno-CdS spectral. (For interpretation of the references to colour in this figure legend, the reader is referred to the Web version of this article.)

concentration (0.05–0.6 μM) and tended to saturate above 0.4 μM in a finite droplet, which confirmed the feasibility of cation exchange amplification in the droplet detection system for quantitative detection. 0.5 μM of Immuno-CdS tags was used in the next experiment. The signal intensity was relative to the size of the droplets controlled by the velocity of the continuous and dispersed phases. In Fig. S4, a series of flow rates of continuous phase including 2.5, 5, 10, and 20 μL min^{-1} and the flow rate of dispersed phase including 0.5, 1, 2.5, 5, and 10 μL min^{-1} were tested to generate the microdroplets in different sizes ranging from 70 to 245 μm. The corresponding fluorescent signals collected in real time in Fig. 3c decreased with the decrease of droplets. However, when the continuous phase velocity and dispersed phase velocity reached 20 μL min^{-1} and 10 μL min^{-1}, respectively, the short interval from droplet formation to detection makes the cation exchange reaction not fully occur, resulting in a low signal collected. Hence, the continuous phase velocity of 10 μL min^{-1} and the dispersed phase velocity of 5 μL min^{-1} were selected to ensure the high flux generation of droplets (~160 μm) and the high efficiency of fluorescence detection. The throughput was approximately 137 droplets per min. Additionally, we collected droplet signals at 10 different positions in the output quartz tube after droplet formation to obtain the optimal detection distance. Fig. 3d was the corresponding fitting curve indicating that the fluorescence signal was correlated with the distance and was stable at more than 5.5 cm. It represents the signal amplification response was completely

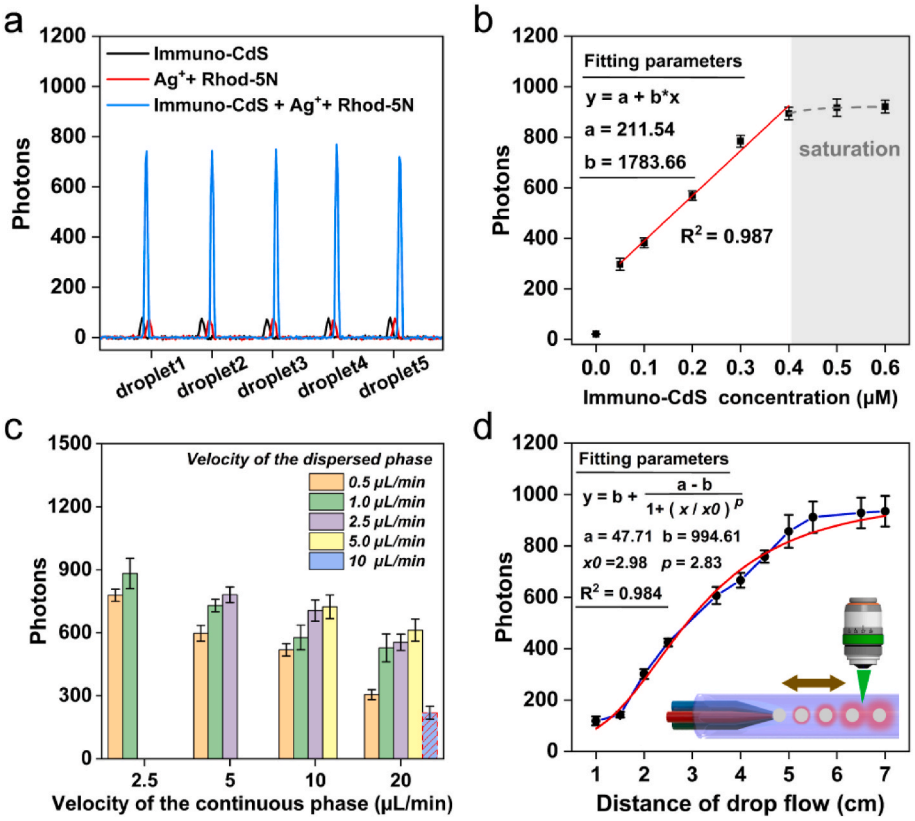

Fig. 3. a) Fluorescence signal of CdS, Rhod-5N before (Ag^+ + Rhod-5N) and after cation exchange reaction (CdS + Ag^+ + Rhod-5N). b) Corresponding calibration lines of Immuno-CdS tags. c) Fluorescence signal of droplets produced by different continuous and dispersed phase velocities. d) Real-time detection of droplets at different positions by PMT. Insert image was the schematic diagram of cation exchange signal amplification reaction process at different detection positions. Error bars indicate the standard deviations calculated from five separate experiments.

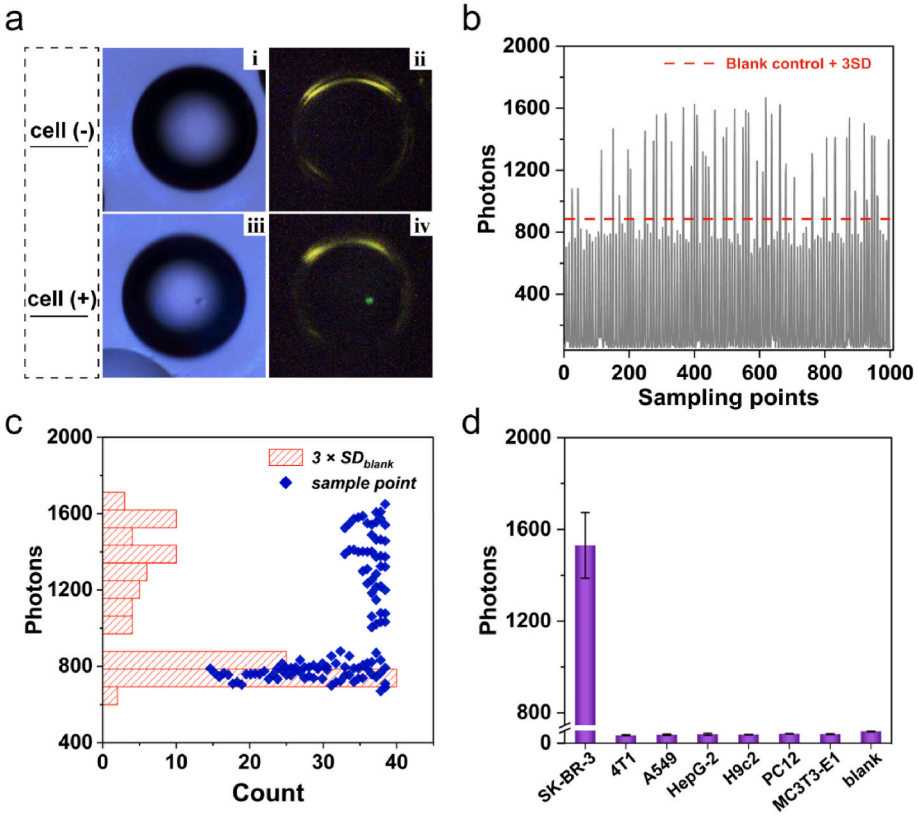

Fig. 4. a) Fluorescence microscopy images of droplets: (i) bright field and (ii) dark field images not containing single cells, (iii) bright field and (iv) dark field images containing single cells. b) The photon number or fluorescence intensity of the moving droplets generated in the droplet microfluidic flow detection system. c) Classification of the photon number. d) Specificity of the droplet microfluidics flow detection system based on cation exchange reaction.

accomplished during 5.5–7 cm, which can be considered the optimal range for signal acquisition. The time required to complete the reaction was the signal acquisition position divided by the flow rate. The instantaneous process from droplet formation to fluorescence detection further reduces the influence of environmental factors on detection results.

3.4. Detection of HER2 protein on single cell

The single-cell detection capability of the droplet microfluidic flow detection system was evaluated by detecting Calcein AM (490 nm excitation wavelength) staining breast SK-BR-3 cells in droplets. The cell suspension was prediluted 10^3 times with PBS buffer (10 mM, pH 7.4) to ensure the number of cells in a droplet was < 1 on average. Fig. 4a was the fluorescence microscope images of droplets with and without containing cells. Notably, only one cell with significant green fluorescence was successfully encapsulated in a droplet, accounting for about 40.35% of all droplets generated in 1min. The cell encapsulation performance ensures autonomous single-cell detection by regulating the concentration of cells before being injected into the capillary bundle, which provide a novel and common platform for detecting biomarker protein in single cells.

Under the optimized detection conditions, the SK-BR-3 cell suspension was used to specifically identify HER2 proteins on the surface of single cells. As displayed in Fig. S5 obtained by confocal laser scanning microscopy (CLSM), the FITC-SA with red fluorescence was clearly distributed around the surface of breast SK-BR-3 cells after the combination of anti-HER2 antibody (Biotin) (Figs. S5a–b), whereas not in the absence of biotin-labeled antibody (Figs. S5c–d). The highly effective binding of specific antibodies suggested that HER2 protein was highly expressed in this cell line. Based on the LOD value of the detection system calculated by the IUPAC formula (LOD = blank control + 3 × SD_{blank}, where blank control and SD_{blank} are the average fluorescence intensity and standard deviation, respectively) from real-time cation exchange amplification signals of blank control droplets produced by different droplet generation chips as shown in Fig. S6, we randomly collected a test group of droplet signals, subsequently. As shown in Fig. 4b, there was a significant difference between the fluorescent signal of the 113 droplets containing a cell and without cells in the sample points generated within 50 ms. By statistical analysis in Fig. 4c, all the droplets were clearly divided into single-cell encapsulation and cell-free encapsulation. Moreover, the signal intensities directly reflect HER2 protein content on the surface of individual cells to a certain degree. The higher expression of the HER2 protein contributes to the more Immuno-CdS tags binding, the higher the fluorescence signal stimulated by cation exchange. We also assessed the specificity of the detection system using several common cell lines with no HER2 protein expression as interferers, including 4T1 (Murine breast cells), A549 (Human lung adenocarcinoma cells), HepG-2 (Human hepatocellular cells), H9c2 (Cardiomyocytes), PC12 (Pheochromocytoma cells) and MC3T3-E1 (Osteoblastic cells). Fig. 4d revealed that all interference groups showed similar fluorescence intensity to the blank control, whereas a distinct signal appeared in the HER2 protein group, indicating the high specificity toward the target biomarkers among cells. Hence, the proposed detection system was capable of simply detecting specific proteins on single-cell and identifying subtle distinctions of target analytes.

3.5. Quantitative detection of HER2 protein in a single cell

To simulate the expression of HER2 protein on a single breast cancer cell membrane, various concentrations of HER2 protein (from 1×10^6 pg mL^{-1} to 0 pg mL^{-1}) were immobilized on carboxylated PS microspheres (diameter 10 μm) surface to incubated with excess Immuno-CdS tags. The preparation process of antigen-modified-PS microspheres was consistent with Immuno-CdS tags. The Zeta potential of PS microspheres decreased with increasing HER2 protein amount in Fig. S7, indicating the completion of PS microsphere model. In this part, according to the pre-experiment of the monodisperse fluorescent PS microspheres (580 nm excitation wavelength) with the same diameter and concentration, encapsulating a single PS microsphere in a droplet could be realized when the PS microspheres concentration is reduced to 0.1‰w/v (Fig. 5a i-iii). And the encapsulation rate was approximately 9.54%, which conformed to the Poisson distribution [41]. The cation exchange amplification fluorescent signal of droplets containing a PS microsphere was randomly real-time collected 20 times and averaged to reduce the sampling errors. As shown in Fig. 5b, the fluorescent intensity decreased gradually with decreasing HER2 protein concentration and was well distinguishable within 0–1×10^6 pg mL^{-1}. Moreover, the fluorescent intensity remarkably correlated linearly with the HER2 protein within the dynamic range of 31.25–1×10^6 pg mL^{-1}. The detection limit of HER2 protein in this experiment was 11.372 pg mL^{-1}, based on calculation with concentration corresponding to three times the standard deviation of the 0 pg mL^{-1} measurement. The HER2 protein on the surface of one cell was roughly quantified by bringing the fluorescent signal of the droplets containing a cell into the linear relationship, distinguished the delicate difference between cells. According to the calculation formula in S3, the maximum and minimum values were 9862.954 pg mL^{-1} and 205.26 pg mL^{-1}, which was equivalent to 9.795×10^6 and 2.038×10^5 biomarker protein molecules in one microdroplet, respectively. And the average of HER2 protein in the droplets containing single cells was 2817.838 pg mL^{-1}, corresponding to 2.798×10^6 molecules, which is consistent with the single-cell level assessment of HER2 expression in tissue sections [42].

We also compared the performance of this cationic amplification system with traditional fluorescent labeling method using the same antibody when applied to carboxyl-activated PS microspheres. As revealed in Fig.5c, the former produced 4.8 times as many fluorescent signals as the latter. And the 4.2 folds RSD interpolation demonstrated the application of cation exchange reaction effectively reduced the relative error caused by the random position of the target analyte in the droplets by releasing the reporter molecules into the droplets for uniform amplified fluorescence. This pattern improved the accuracy of cation exchange-based droplet microfluidic system detection.

Compared to other recently reported biosensors for HER2 protein detection, our proposed droplet microfluidics chip based on the cation exchange amplification achieved single-cell autonomous detection and performed better in sensitivity and quantification (Table 1). Moreover, this method of obtaining standard curves from microsphere simulations allows quantitative detection of other important biomarkers on the cell surface. It is of great significance in the quantitative analysis of cancer cell-specific proteins or other single-cell analysis fields. However, there are still barriers to detecting tiny droplets (less than 50 μm), such as those containing bacteria. Further improvement of fluorescence collection method and efficiency can make it a common platform for single cell detection.

4. Conclusion

In this work, we proposed a novel microfluidic droplet-based fluorescence amplification detection system for single breast cancer cell detection via cation exchange reaction. After modification with specific HER2 antibodies, CdS QDs densely adhered to the target cell surface. A large number of Cd^{2+} was exchanged instantaneously by cation exchange reaction, and combined with Rhod-5N distributed evenly in droplets to obtain amplified and stable fluorescence signals. The detection system can perform instantaneous detection from reagents mixing to signal amplification to avoid the influence of complex environments on cells. In terms of detection, the LOD of HER2 protein determined from droplets encapsulated single PS microsphere was as low as 11.372 pg mL^{-1}. The fluorescence signal of HER2 protein on the cell surface can be converted into the corresponding concentration through the calibration line, ranging from 9.795×10^6 and 2.038×10^5

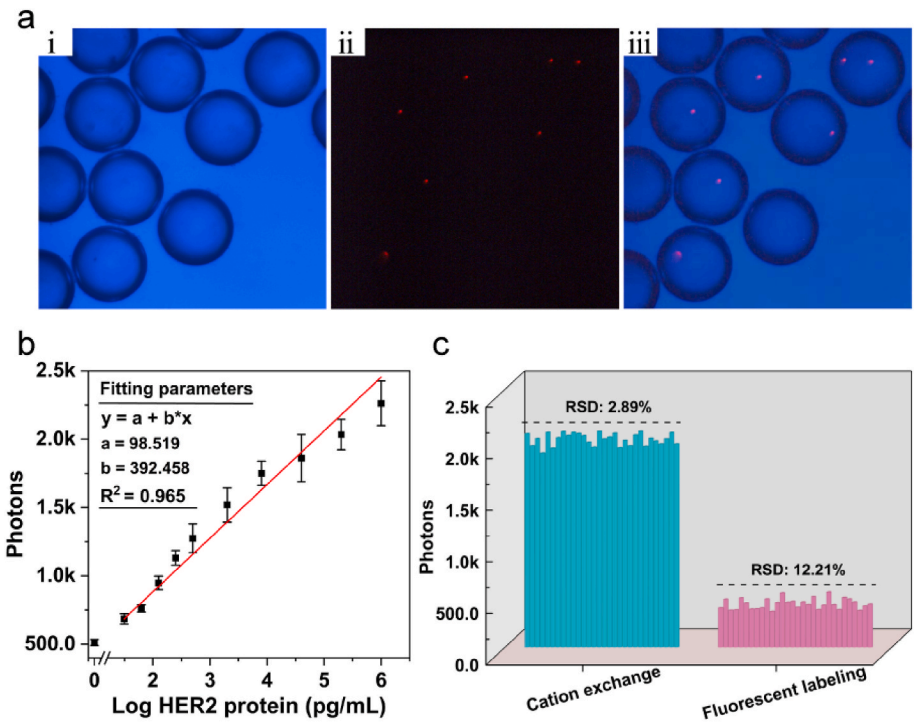

Fig. 5. a) Fluorescence microscopy images of fluorescent PS microspheres wrapped in droplets: (i) bright imaging, (ii) dark-field imaging and (iii) bright field, and dark field overlap imaging. b) Calibration line of different concentrations of HER2 protein modified on PS microspheres. c) Comparison between fluorescence detection of cation exchange reaction and fluorescent labeling method in droplets using PS microspheres.

Table 1
Characteristics of the cation exchange-based droplet microfluidic flow detection system compared with other recently reported HER2 protein detection techniques.

Detection technique	Target	Detection characteristics	Reference
Immunofluorescence	single-cell level on FFPE patient samples	Quantification of HER2 expressing level	Onsum et al., 2013 [42]
LC-MS/MS-based proteomics	HER2-positive breast cancer cells	LOQ: 25 pmol L^{-1}	Zhou et al., 2018 [43]
Electrochemical immunosensor	HER2 proteins	LOD: 0.28 ng mL^{-1}	Lah et al., 2019 [44]
Electrochemical immunosensor	Human serum	LOD: 45 pg mL^{-1}	Wang et al., 2021 [45]
Optical sensor (SPR)	HER2 proteins	LOD: 0.6 μg mL^{-1} in label-free, 9.3 ng mL^{-1} in label	Loyez et al., 2021 [46]
Abs-Lu probes-based SC-ICP-MS	individual cells	Distinguish between HER2 negative and positive cells	Asensio et al., 2021 [47]
Cation exchange-based droplet microfluidic	**individual cells**	**LOD:** 11.372 pg mL^{-1}, Quantification of HER2 protein on the cell surface	**This work**

protein molecules. The high performance of the instant cation exchange signal amplification-microdroplet system in trace detection of single-cell protein surface proteins makes it promising to be a powerful tool for the study of intracellular heterogeneity and diagnosis of tumor subtypes.

CRediT authorship contribution statement

Xiaoxian Liu: Preparation of droplet generation chip, Experiment, Data curation, Writing-results. **Yifan Zhu:** Preparation of droplet generation chip, Experiment. **Caoxin Li:** Preparation of droplet generation chip, Experiment. **Yanyun Fang:** Culture and quantification of cells. **Jinna Chen:** Writing – review & editing. **Fei Xu:** Fiber tip cutting and preparation. **Yanqing Lu:** Writing – review & editing. **Perry Ping Shum:** Writing – review & editing. **Ying Liu:** Writing – review & editing. **Guanghui Wang:** Experiment design, Writing – review & editing.

Declaration of competing interest

The authors declare that they have no known competing financial interests or personal relationships that could have appeared to influence the work reported in this paper.

Data availability

Data will be made available on request.

Acknowledgment

This work was sponsored by the National Natural Science Foundation of China (nos. 61875083, 61535005), and Social Development Project of Jiangsu Province (BE2019761). The authors Xiaoxian Liu, Yifan Zhu, and Caoxin Li contributed equally to this work.

Appendix A. Supplementary data

Supplementary data to this article can be found online at https://doi.org/10.1016/j.aca.2023.340976.

References

[1] H. Sung, J. Ferlay, R.L. Siegel, M. Laversanne, I. Soerjomataram, A. Jemal, F. Bray, Global cancer statistics 2020: GLOBOCAN estimates of incidence and mortality worldwide for 36 cancers in 185 countries, CA A Cancer J. Clin. 71 (2021) 209–249.
[2] R.L. Siegel, K.D. Miller, H.E. Fuchs, A. Jemal, Cancer statistics, 2022, CA A Cancer J. Clin. 72 (2022) 7–33.

[3] N. Harbeck, M. Gnant, Breast cancer, Lancet 389 (2017) 1134–1150.
[4] C. Thomssen, M. Balic, N. Harbeck, M. Gnant, St Gallen/Vienna, A brief summary of the consensus discussion on customizing therapies for women with early breast cancer, Breast Care 16 (2021) 135–143.
[5] A.C. Wolff, M.E. Hammond, D.G. Hicks, M. Dowsett, L.M. McShane, K.H. Allison, et al., Recommendations for human epidermal growth factor receptor 2 testing in breast cancer: American Society of Clinical Oncology/College of American Pathologists clinical practice guideline update, J. Clin. Oncol. 31 (2013) 3997–4013.
[6] A. Perrier, J. Gligorov, G. Lefevre, M. Boissan, The extracellular domain of Her2 in serum as a biomarker of breast cancer, Lab. Invest. 98 (2018) 696–707.
[7] C. Mueller, A. Haymond, J.B. Davis, A. Williams, V. Espina, Protein biomarkers for subtyping breast cancer and implications for future research, Expert Rev. Proteomics 15 (2018) 131–152.
[8] R. Salahandish, A. Ghaffarinejad, S.M. Naghib, A.K. Majidzadeh, H. Zargartalebi, A. Sanati-Nezhad, Nano-biosensor for highly sensitive detection of HER2 positive breast cancer, Biosens. Bioelectron. 117 (2018) 104–111.
[9] S. Ahn, J.W. Woo, K. Lee, S.Y. Park, HER2 status in breast cancer: changes in guidelines and complicating factors for interpretation, J Pathol Transl Med 54 (2020) 34–44.
[10] J. Wagner, M.A. Rapsomaniki, S. Chevrier, T. Anzeneder, C. Langwieder, A. Dykgers, et al., A single-cell atlas of the tumor and immune ecosystem of human breast cancer, Cell 177 (2019) 1330–1345 e18.
[11] N.V. Jordan, A. Bardia, B.S. Wittner, C. Benes, M. Ligorio, Y. Zheng, et al., HER2 expression identifies dynamic functional states within circulating breast cancer cells, Nature 537 (2016) 102–106.
[12] X. Li, B. Fan, S. Cao, D. Chen, X. Zhao, D. Men, W. Yue, J. Wang, J. Chen, A microfluidic flow cytometer enabling absolute quantification of single-cell intracellular proteins, Lab Chip 17 (2017) 3129–3137.
[13] Y. Ahn, B. Gibson, A. Williams, P. Alusta, D.A. Buzatu, Y.J. Lee, et al., A comparison of culture-based, real-time PCR, droplet digital PCR and flow cytometric methods for the detection of Burkholderia cepacia complex in nuclease-free water and antiseptics, J. Ind. Microbiol. Biotechnol. 47 (2020) 475–484.
[14] S.M. Manohar, P. Shah, A. Nair, Flow cytometry: principles, applications and recent advances, Bioanalysis 13 (2021) 181–198.
[15] G.M. Whitesides, The origins and the future of microfluidics, Nature 442 (2006) 368–373.
[16] X. Wang, S. Chen, M. Kong, Z. Wang, K.D. Costa, R.A. Li, D. Sun, Enhanced cell sorting and manipulation with combined optical tweezer and microfluidic chip technologies, Lab Chip 11 (2011) 3656–3662.
[17] W.M. Weaver, P. Tseng, A. Kunze, M. Masaeli, A.J. Chung, J.S. Dudani, H. Kittur, R.P. Kulkarni, D. Di Carlo, Advances in high-throughput single-cell microtechnologies, Curr. Opin. Biotechnol. 25 (2014) 114–123.
[18] A. Reece, B. Xia, Z. Jiang, B. Noren, R. McBride, J. Oakey, Microfluidic techniques for high throughput single cell analysis, Curr. Opin. Biotechnol. 40 (2016) 90–96.
[19] T. Luo, L. Fan, R. Zhu, D. Sun, Microfluidic single-cell manipulation and analysis: methods and applications, Micromachines 10 (2019).
[20] N. Wen, Z. Zhao, B. Fan, D. Chen, D. Men, J. Wang, J. Chen, Development of droplet microfluidics enabling high-throughput single-cell analysis, Molecules 21 (2016).
[21] Y. Zhu, G. Clair, W.B. Chrisler, Y. Shen, R. Zhao, A.K. Shukla, et al., Proteomic analysis of single mammalian cells enabled by microfluidic nanodroplet sample preparation and ultrasensitive NanoLC-MS, Angew Chem. Int. Ed. Engl. 57 (2018) 12370–12374.
[22] T. Khajvand, P. Huang, L. Li, M. Zhang, F. Zhu, X. Xu, et al., Interfacing droplet microfluidics with antibody barcodes for multiplexed single-cell protein secretion profiling, Lab Chip 21 (2021) 4823–4830.
[23] F.V. De Rop, J.N. Ismail, C.B. González- Blas, G.J. Hulselmans, Hydrop enables droplet- based single- cell ATAC- seq and single- cell RNA- seq using dissolvable hydrogel beads, Elife 11 (2022), e73971.
[24] L. Mazutis, J. Gilbert, W.L. Ung, D.A. Weitz, A.D. Griffiths, J.A. Heyman, Single-cell analysis and sorting using droplet-based microfluidics, Nat. Protoc. 8 (2013) 870–891.
[25] B. Fan, X. Li, D. Chen, H. Peng, J. Wang, J. Chen, Development of microfluidic systems enabling high-throughput single-cell protein characterization, Sensors 16 (2016) 232.
[26] D. Liu, M. Sun, J. Zhang, R. Hu, W. Fu, T. Xuanyuan, W. Liu, Single-cell droplet microfluidics for biomedical applications, Analyst 147 (2022) 2294–2316.
[27] A. Hassanzadeh-Barforoushi, M.E. Warkiani, D. Gallego-Ortega, G. Liu, T. Barber, Capillary-assisted microfluidic biosensing platform captures single cell secretion dynamics in nanoliter compartments, Biosens. Bioelectron. 155 (2020), 112113.
[28] L. Mei, M. Jin, S. Xie, Z. Yan, X. Wang, G. Zhou, A. van den Berg, L. Shui, A simple capillary-based open microfluidic device for size on-demand high-throughput droplet/bubble/microcapsule generation, Lab Chip 18 (2018) 2806–2815.
[29] R.R. Hood, T. Wyderko, D.L. DeVoe, Programmable digital droplet microfluidics using a multibarrel capillary bundle, Sensor. Actuator. B Chem. 220 (2015) 992–999.
[30] S. Liao, X. Tao, Y. Ju, J. Feng, W. Du, Y. Wang, Multichannel dynamic interfacial printing: an alternative multicomponent droplet generation technique for lab in a drop, ACS Appl. Mater. Interfaces 9 (2017) 43545–43552.
[31] D. Leng, J. Zhao, X. Ren, R. Xu, L. Liu, X. Liu, Y. Li, Q. Wei, MoSe2/CdSe heterojunction destruction by cation exchange for photoelectrochemical immunoassays with a controlled-release strategy, Anal. Chem. 93 (2021) 10712–10718.
[32] H. Xu, X. Niu, Z. Liu, M. Sun, Z. Liu, Z. Tian, et al., Highly controllable hierarchically porous Ag/Ag2 S heterostructure by cation exchange for efficient hydrogen evolution, Small 17 (2021), e2103064.
[33] Y. Guo, Z. Liang, Y. Xue, X. Wang, X. Zhang, J. Tian, A cation exchange strategy to construct Rod-shell CdS/Cu2S nanostructures for broad spectrum photocatalytic hydrogen production, J. Colloid Interface Sci. 608 (2022) 158–163.
[34] Z. Sheng, D. Hu, P. Zhang, P. Gong, D. Gao, S. Liu, L. Cai, Cation exchange in aptamer-conjugated CdSe nanoclusters: a novel fluorescence signal amplification for cancer cell detection, Chem. Commun. 48 (2012) 4202–4204.
[35] J. Yao, K. Flack, L. Ding, W. Zhong, Tagging the rolling circle products with nanocrystal clusters for cascade signal increase in the detection of miRNA, Analyst 138 (2013) 3121–3125.
[36] L. Wu, Y. Wang, R. He, Y. Zhang, Y. He, C. Wang, Z. Lu, Y. Liu, H. Ju, Fluorescence hydrogel array based on interfacial cation exchange amplification for highly sensitive microRNA detection, Anal. Chim. Acta 1080 (2019) 206–214.
[37] Y. Zhao, X. Cai, C. Zhu, H. Yang, D. Du, A novel fluorescent and electrochemical dual-responsive immunosensor for sensitive and reliable detection of biomarkers based on cation-exchange reaction, Anal. Chim. Acta 1096 (2020) 61–68.
[38] J. Xu, Q.M. Zhang, D.X. Zhao, Y.R. Liu, P. Chen, G.H. Lu, H.Y. Xie, High sensitive detection method for protein by combining the magnetic separation with cation exchange based signal amplification, Talanta 168 (2017) 91–99.
[39] E. Han, L. Ding, S. Jin, H. Ju, Electrochemiluminescent biosensing of carbohydrate-functionalized CdS nanocomposites for in situ label-free analysis of cell surface carbohydrate, Biosens. Bioelectron. 26 (2011) 2500–2505.
[40] X. Liu, X. Yang, K. Li, H. Liu, R. Xiao, W. Wang, C. Wang, S. Wang, Fe3O4@Au SERS tags-based lateral flow assay for simultaneous detection of serum amyloid A and C-reactive protein in unprocessed blood sample, Sensor. Actuator. B Chem. 320 (2020).
[41] A. Link, J.S. McGrath, M. Zaimagaoglu, T. Franke, Active single cell encapsulation using SAW overcoming the limitations of Poisson distribution, Lab Chip 22 (2021) 193–200.
[42] M.D. Onsum, E. Geretti, V. Paragas, A.J. Kudla, S.P. Moulis, L. Luus, et al., Single-cell quantitative HER2 measurement identifies heterogeneity and distinct subgroups within traditionally defined HER2-positive patients, Am. J. Pathol. 183 (2013) 1446–1460.
[43] W. Zhou, F. Xu, D. Li, Y. Chen, Improved detection of HER2 by a quasi-targeted proteomics approach using aptamer-peptide probe and liquid chromatography-tandem mass spectrometry, Clin. Chem. 64 (2018) 526–535.
[44] Z. Lah, S.A.A. Ahmad, M.S. Zaini, M.A. Kamarudin, An electrochemical sandwich immunosensor for the detection of HER2 using antibody-conjugated PbS quantum dot as a label, J. Pharm. Biomed. Anal. 174 (2019) 608–617.
[45] W. Wang, R. Han, M. Chen, X. Luo, Antifouling peptide hydrogel based electrochemical biosensors for highly sensitive detection of cancer biomarker HER2 in human serum, Anal. Chem. 93 (2021) 7355–7361.
[46] M. Loyez, M. Lobry, E.M. Hassan, M.C. DeRosa, C. Caucheteur, R. Wattiez, HER2 breast cancer biomarker detection using a sandwich optical fiber assay, Talanta 221 (2021), 121452.
[47] A.F. Asensio, M. Corte-Rodriguez, J. Bettmer, L.M. Sierra, M. Montes-Bayon, E. Blanco-Gonzalez, Targeting HER2 protein in individual cells using ICP-MS detection and its potential as prognostic and predictive breast cancer biomarker, Talanta 235 (2021), 122773.